Synthesis of oligosaccharide libraries from GBS capsular polysaccharides for structure-based selection of vaccine candidates

Del Bino, L.

Chapter 7

Structure guided design of a fully synthetic GBS type III glycoconjugate vaccine

Oldrini, D.; Del Bino, L.; Ardà, A.; Carboni, F.; Angiolini, F.; Quintana, J.I.; Calloni, I.; Romano, M.R.; Berti, F.; Margarit y Ros, I.; Jiménez-Barbero, J.; Adamo, R. *Chem. Eur. J.*, **2020**, https://doi.org/10.1002/chem.202000284

Introduction

Among the 10 different serotypes of GBS, type III is the most prevalent serotype causing infections[1]. As mentioned, GBS infections in infants can occur within six days from the delivery, and in this case they are called Early-Onset Diseases (EOD), or after the first week of life up to three months of age (Late-OnSet Diseases, LOD)[2].

More than 90% of EOD are caused by serotypes Ia, Ib, II, III, and V, while LODs are caused predominantly by serotype III[3]. GBS infections can also occur in elderly or immunocompromised patients. In adults, serotype V (27.5%) was shown to be a predominant serotype, followed by Ia (24.3%) and III (16.5%)[4, 5].

GBS capsular polysaccharides are the main targets for vaccine development. However, purified GBS PSs are only variably immunogenic in adults, therefore PS–protein conjugate vaccines have been developed to enhance their immunogenicity[6, 7].

PSIII repeating unit is composed of pentasaccharide shown on Figure 1[8]:

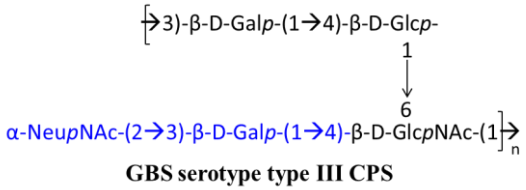

Figure 1. Repeating unit of GBS serotype III capsular polysaccharide

GBS PSIII glycoconjugates have been tested, alone and in combination with PS Ia and Ib conjugates in a trivalent formulation, in Phase I/II clinical trials and proven to be safe, well-tolerated and to elicit functionally active antibodies which are transferred to the baby through the placenta[9].

Although bacterial surface polysaccharides are often optimal target for vaccine discovery, structural details of the antigenic determinants responsible for their binding to specific functional antibodies are unknown[10].

GBS type III PS has been exceptionally studied (also compared to other GBS serotypes) and has been proposed as the prototype of a unique length-dependent conformational epitope. Molecular dynamics simulations and NMR studies[11, 12] showed that the GBS PSIII is flexible in solution and predominantly exists as a random coil. However, more than four repeating units (RUs) are able to form extended helical structures stabilized by the presence of the charged sialic acid residues[13, 14]. On the other hand, the structurally related *Streptococcus pneumoniae* type 14 polysaccharide, which differs from PSIII by the absence of the Neu5Ac, results in a more disordered structure[15]. Furthermore, a high affinity monoclonal antibody (mAb) specific to PSIII was found, and PS fragments of different size were recognized by the anti-PSIII mAb in a length dependent manner. A dimer of 2RUs (Figure 3) was shown to be sufficient to bind to a monoclonal IgG, although

with much lower affinity as compared to fragments composed of a larger number of RUs[14]. These properties have been rationalized in terms of the presence of a conformational epitope situated on an extended segment of the GBS PSIII[16-18].

Recently, three different sequences, one linear glycan (**1**) and the two branched structures **2** and **3**, corresponding to GBS PSIII repeating units, were prepared (Figure 2)[19].

The three synthesized structures where conjugated to Cross Reacting Material 197 (CRM_{197}), and competitive ELISA with anti GBS PSIII serum showed the importance of the branching formed motif Glc*p*-(1→6)-Glc*p*NAc for antibody recognition. These structures, together with fragments obtained from PS depolymerization, were also used to define the molecular details of the interactions with anti-PSIII mAbs by STD-NMR and X-ray crystallography[10]. Carboni et al. demonstrated the existence of a sialic acid-dependent functional epitope in GBS III where most of the contact area with the Fab involves a single repeating unit; the minimal binding structure contains four consecutive sugars composing the PSIII backbone and one disaccharide present in the branching (Figure 3). The dimer obtained by polysaccharide depolymerization was shown immunogenic after conjugation to the carrier protein[20].

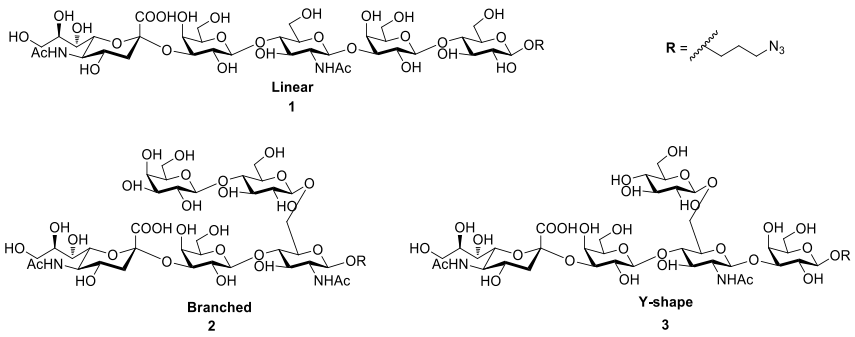

Figure 2. Linear, branched and Y-shape frameshifts of GBS serotype III repeating unit

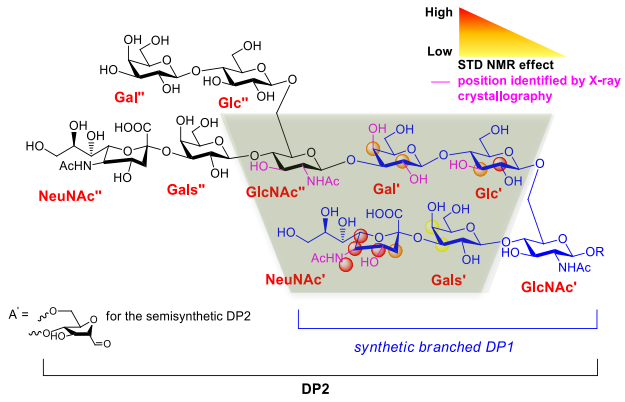

Figure 3. GBS PSIII epitope mapping with 2 RU semi-synthetic fragment. Protons interacting with the mAb identified by STD-NMR and X-ray crystallography.

This Chapter describes on the basis of the X-Ray crystallographic structure of the dimer-Fab complex, the design of a hexasaccharide comprising the residues involved in the binding of the polysaccharide with the protective mAb. Next to this, the synthesis of this hexasaccharide is outlined, followed by a study of the interactions between the hexasaccharide and a protective anti PSIII rabbit mAb by competitive Surface Plasmon Resonance and Saturation Transfer Difference NMR (SDT-NMR). The obtained results were corroborated by Molecular Dynamics simulation and NMR experiments comparing the conformation of the hexasaccharide in the binding pocket of the anti PSIII Fab to the one of the semisynthetic DP2 of the published X-Ray crystal structure (pdb 5m6).

Results

Starting from the previously described structural results, the use of a structure-guided approach was envisaged to design the small hexasaccharide **4** comprising all sugar moieties directly interacting with mAb binding pocket as a minimal immunogenic epitope (Scheme 1).
Compound **4**, bearing a linker at the reducing end for conjugation to a carrier protein, was chemically synthesized by conventional carbohydrate chemistry procedures. To do so, known trisaccharide **6**[19] was elongated with lactose donor **5** bearing a participating protecting group at position 2 to give pentasaccharide **7**, that was subjected to acid hydrolysis. The free C3 and C4 hydroxyl groups in the galactose residue of obtained **8** set the stage for a regioselective glycosylation at Gal C-3 (see Chapter 3) with donor **9** to give the fully protected hexamer **10**. The final stage, in which all protecting groups in **10** were removed, consists of the following five step: (i) removal of the methyl ester of Neu5Ac with lithium iodide in pyridine; (ii) reaction with ethylenediamine in refluxing ethanol for concomitant removal of the *O*-acetates and the *N*-Phth protecting group; (iii) reacetylation with acetic anhydride/pyridine to install the acetamide group of the GlcNAc residues along with acetyl esters; (iv) methanolysis and v) final catalytic hydrogenation over Pd/charcoal to provide the target branched hexasaccharide **4**, which was desalted and characterized.

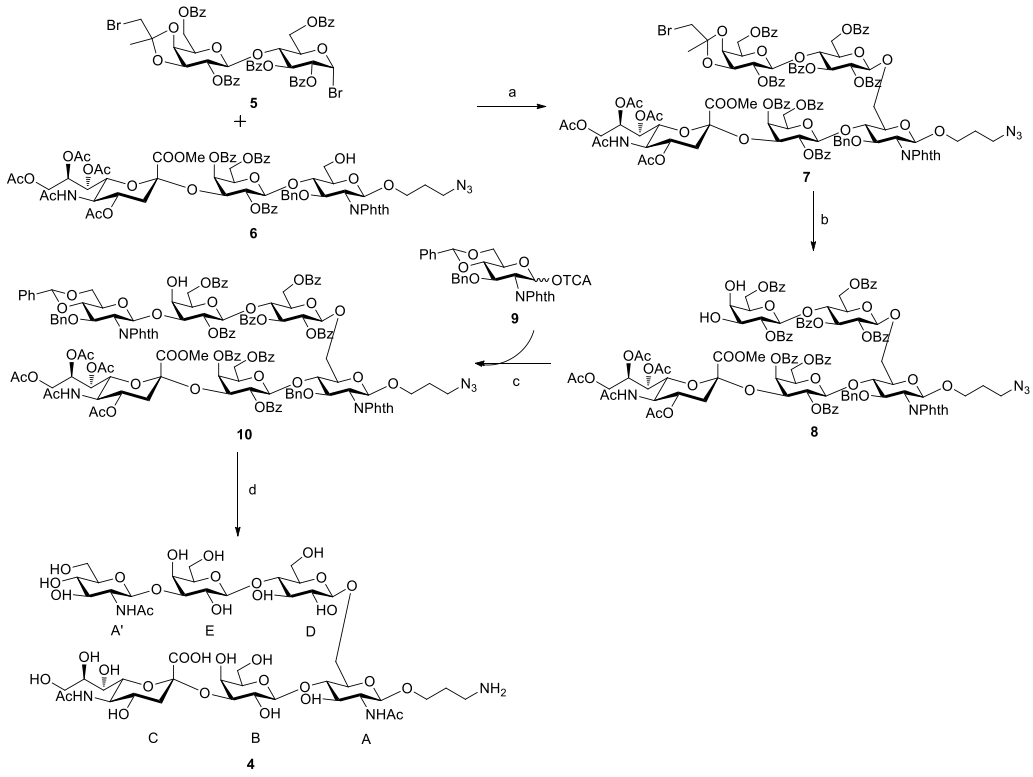

Scheme 1. *Reagents and conditions*: a) AgOTf, dry DCM, -10°C, 65%; b) 9:1 TFA-H_2O, 80%; c) TMSOTf, dry DCM, -30°C, 69%; d) LiI, Py, 120°C; $H_2NCH_2CH_2NH_2$, EtOH, 90°C; Ac_2O, Py; MeONa, MeOH; H_2, Pd-C, 40% (over five steps).

With hexasaccharide **4** in hand, it was investigated whether this structure corresponds to a minimal immunogenic epitope of GBS III.

The capacity of the hexasaccharide **4** to cover the determined epitope was evaluated by competitive SPR by which its ability as an inhibitor of the binding of a soluble Fab fragment to PSIII conjugated to Human Serum Albumin (HSA) immobilized on a chip was assessed.

The hexasaccharide showed an affinity 2 orders of magnitude higher than the branched structure and fully mimicking the semisynthetic PSIII dimer DP2. This result confirmed that only the upstream GlcNAc **A'** is engaged in interactions with the mAb, while the downstream end GlcNAc **A**, which was replaced by a mannofuranoside in the crystallized semisynthetic glycan, is not accommodated in the binding pocket (Figure 4A).

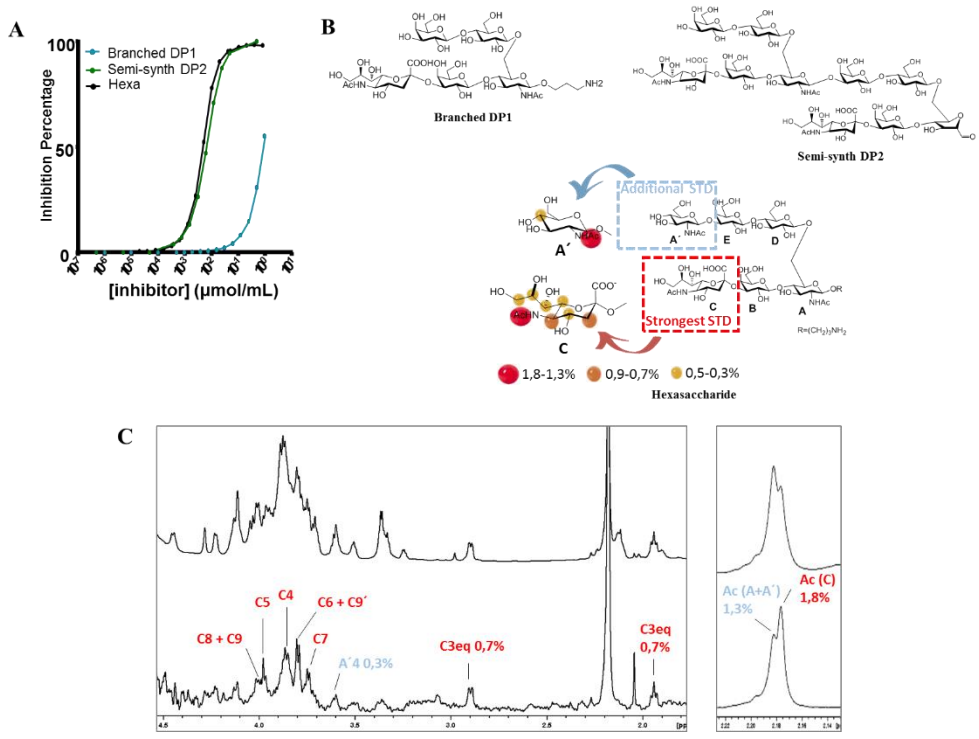

Figure 4. A) Competitive SPR against an anti PSIII rabbit Fab of the branched DP1, the semisynthetic DP2 and the hexasaccharide. B) Structure of the tested oligosaccharides and STD-NMR interpretation: mapping of the hexasaccharide protons more closely interacting with the mAb. C) ^{1}H-STD-NMR experiment: off-resonance (top) and STD (below) spectra for the hexasaccharide **4** interacting with mAb, with a zoom on N-acetyl signals on the right. Proton positions receiving strongest saturation after protein irradiation (STD effect) are indicated in red, and isolated proton signals with weaker STD are in blue.

A more detailed ligand-mAb interaction analysis was carried out by STD-NMR (Figure 4B/C)[21, 22]. Most of the peaks in the STD-NMR correspond to signals related to Neu5NAc and to Gal' in the branch, confirming that Neu5Ac is a major anchoring site for mAb interaction. Notably, the peak at 2.03 ppm, corresponding to the NAc moiety of sialic acid, received the highest transfer of saturation, as compared to the two NAc signals of GlcNAc overlapping at 2.04 ppm. In the ^{1}H NMR, these two NAc moieties showed a ratio of 2:1 with respect to the sialic acid NAc, while in the STD-NMR analysis, the intensity of the peaks at 2.04 and 2.03 ppm was comparable.

These results show that the identified hexasaccharide was interacting with Fab similarly to the dimer obtained by depolymerization previously used for crystallography. To further corroborate this conclusion, a Molecular Dynamics simulation of the hexasaccharide-Fab complex was performed to provide insights on how the synthetic fragment is accommodated in the binding pocket of the mAb.

First, an NMR experiment was carried out to compare the conformational preferences of the hexasaccharide in its free and bound forms. For the free state, the NOESY spectrum was analyzed

and all NOE cross peaks were negative. With respect to interglycosidic flexibility, special attention was payed to the linkage Neu5Acα2-3Gal. A conformational ensemble involving three conformations is present for this flexible linkage (Fig. 5A, left): POP1, where φ/ψ values are ca. 180^0/-20^0, and POP2 and POP3, in a close region of the conformational map, with φ/ψ values ca. -90^0/-50^0, and -65^0/-10^0, respectively.

Inter-residue distances were estimated form the intensities of the NOE cross peaks. Experimentally (Fig. 5B, right), the strong H3ax Neu5Ac(C) – H3 Gal(B) NOE yielded an estimated distance of 2.9Å suggesting the existence of a conformational equilibrium in solution, with the participation of more than one conformation. Indeed, for POP1 conformation, this distance is below 2.5Å, while for the two other energy minima, POP2 and POP3, this distance is 3.6 Å and 4.2 Å respectively. A similar evaluation was done for the interaction of H8 Neu5Ac(C) - H3 Gal(B), which yields an estimated distance of 3.4 Å. This distance is around 4.1 Å in POP1 and 2.6-2.7 Å for POP2 and POP3, corroborating the flexibility around the Neu5Acα2-3Gal linkage.

Interestingly, the situation is different in the trNOESY spectrum (Fig. 5B, left). In this case, the only observable NOEs for H3axNeu5Ac(C) are the intraresidual ones with H4 and H5, while the inter-residue contacts are absent. On the contrary, the NOE between H3eqNeu5Ac(C)–H4Gal(B) is more intense in the trNOESY than in the NOESY, yielding an estimated distance for the bound conformation of 2.7 Å.

These data clearly indicate that there is a conformational selection process upon binding. In particular, in the bound conformation, H3-Gal is oriented towards the glycerol chain of the Neu5Ac residue, such as in POP2 and POP3, while the POP1 conformation has disappeared.

However, the trNOESY analysis do not permit to quantitatively define the torsion angles.

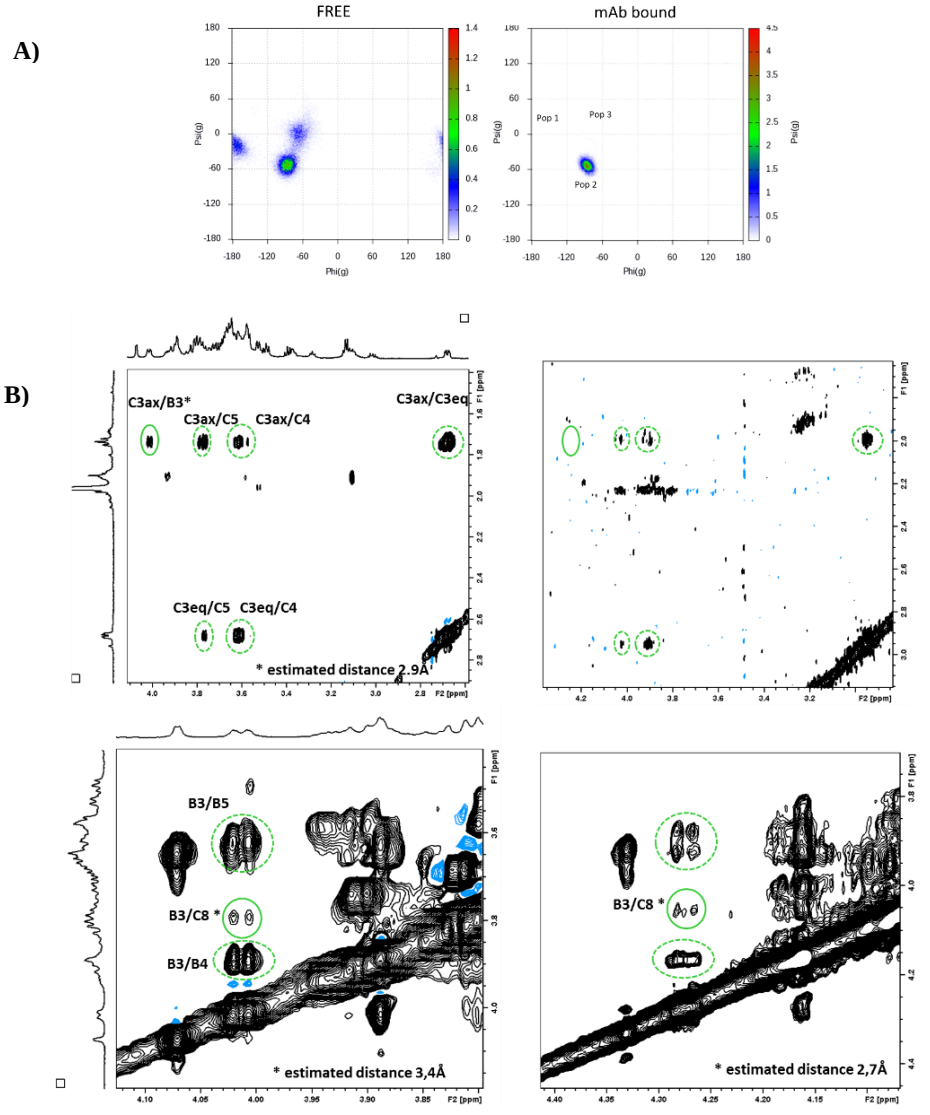

Figure 5. A) MD simulations of Neu5Acα2→3Gal linkage in the hexasaccharide in the free and bound state B) Comparison of the same regions in the NOESY spectrum of the hexasaccahride free (left) (800MHz) and trNOESY of the hexasaccharide in the presence of the mAb (right) (600MHz).

Thus, a Molecular Dynamics (MD) simulation was performed using this geometry as starting structure for the Neu5Acα2-3Gal fragment. The result of the MD simulation is shown in Fig. 6A, which also shows the superimposition of different frames of the ligand bound to the mAb. A single frame for the complex is shown in Fig. 6B.

The hexasaccharide complexed with the mAb shows that the ligand exclusively populates the POP2 region (Fig. 6B right), with a minimum centered at $-90^0/-50^0$. Interestingly, this value is in

perfect agreement with the X-ray crystallographic structure of the fragment DP2 complexed with the mAb (pdb 5m63) for which the φ/ψ values around Neu5Acα2-3Gal are $-80^0/-16^0$.
The Neu5Ac residue establishes different intermolecular hydrogen bonds with polar amino acid chains of the protein. In particular, the carboxylate group at C1, the carbonyl moiety of NHCOMe at C5, and the hydroxyl group at C4 are involved in interactions. On the other hand, the Me group of the NHCOMe is buried into a mAb groove and stacked against the aromatic rings of Y52 and Y115 of the light chain. Interestingly, the carbonyl group of the NHCOMe of the GlcNAc A´ residue also establishes hydrogen bonds with N55 and R66 of the light chain, while the Me group is stacked against Y126 of the heavy chain.

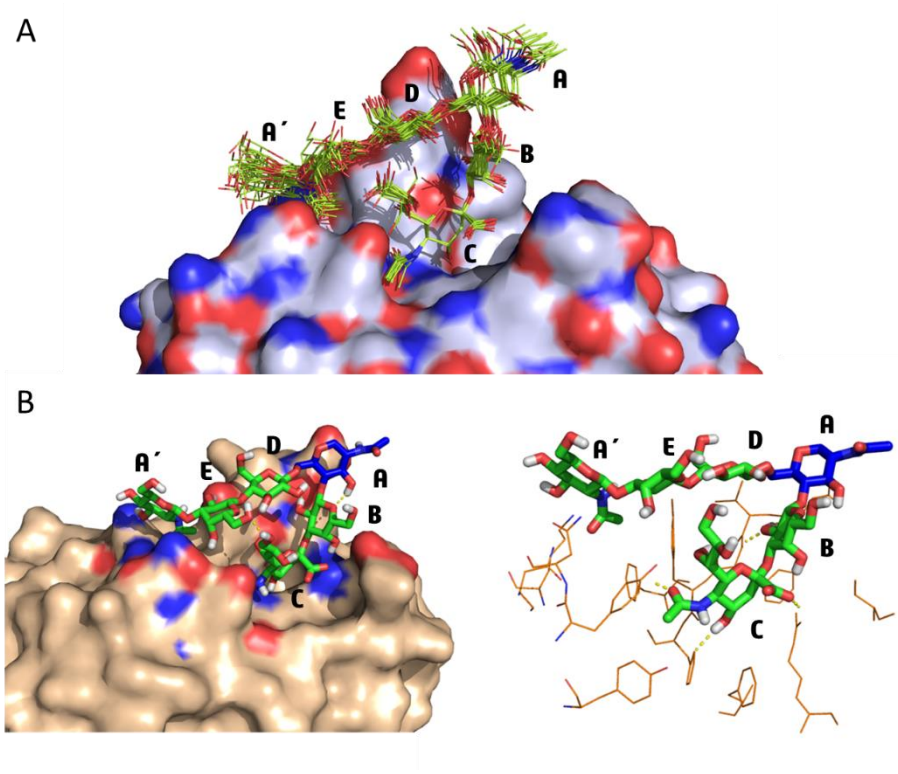

Figure 6. A) Result of the MD simulation: superimposition of different frames of the ligand bound to the mAb is shown. B) A single frame for the complex is shown.

The complex between the hexasaccharide and the mAb obtained by NMR and MD was then compared to the X-ray crystallography structure complex of DP2 with the mAb previously reported (pdb 5m63). Superimposition (Figure 7) shows that both complexes are very similar and share the main interaction points described above. Major differences involve the orientation of residue D (highlighted in red in Figure 7). In the DP2 complex, the ring O5 oxygen and hydroxymethyl group of residue D are pointing towards residue C, while in the hexasaccharide

complex described herein, the pyranose ring is turned 180^0 with respect to that conformation. Consequently, the glycosidic linkages involving this residue are different for both complexes. For the linkage E-D the DP2 complex is in an unusual non-exoanomeric ($-16^0/-118^0$) conformation conformation, while in the hexasaccharide complex, standard exo-anomeric/syn values are obtained($40^0/20^0$). Moreover, for the D-A linkage, the DP2 complex displays a non-exo-anomeric $-47^0/78^0$ conformation, while the hexasaccharide shows a regular $30^0/-160^0$ geometry.

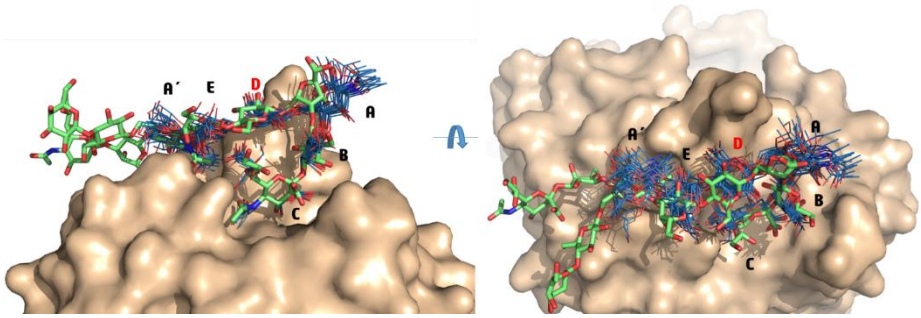

Figure 7. Superimposition of the complex between the hexasaccharide and the mAb and the X-ray crystallography-based complex of DP2 with the mAb already reported (pdb 5m63)

Having established that hexasaccharide **4** contains the moieties related to the minimal antigenic determinant, immunization study with the hexasaccharide conjugated to the well-known carrier protein CRM_{197} was planned to understand whether this small glycan was also behaving as minimal polysaccharide epitope.

It is well-know that multivalence is a crucial attribute in obtaining strong immunogenicity with such small fragments[23, 24]. To this aim, two hexasaccharide conjugates differing in their glycosylation degree were generated. The amino-propyl linker of the hexasaccharide was therefore activated by treatment with an excess of di-N-hydroxysuccinimidyl adipate (Scheme 2)[25]. The isolated activated ester was incubated with the carrier protein CRM_{197} in sodium phosphate buffer at pH 7.2. The amount of coupled glycan was proportional to the active ester used in conjugation (Table 1). Thus, the use of 15 equivalents led to incorporation of an average of 3.9 glycan moieties; when 50 equivalents were used the level of carbohydrate incorporation was increased to 7.8 mol/mol of protein. Glycoconjugates were purified by filtration against sodium phosphate buffer and characterized by 4–12 % sodium dodecyl sulfate polyacrylamide gel electrophoresis (SDS-PAGE) to estimate the carbohydrate/protein molar ratio and by microBCA for the protein content quantification. The degree of carbohydrate incorporation was then corroborated by quantification of the galactose moieties present in the conjugated saccharide through high-performance anion-exchange chromatography coupled with pulsed amperometric detection (HPAEC-PAD)[26].

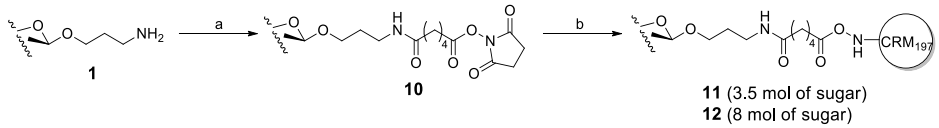

Scheme 2. *Reagents and conditions*: a) Di-N-hydroxysuccinimidyl adipate, triethylamine, DMSO; b) 100mM sodium phosphate 7.2.

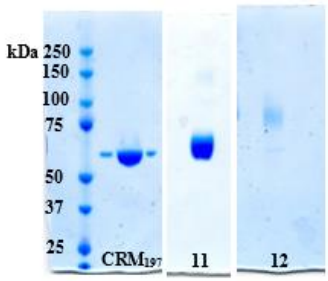

Figure 8. SDS-PAGE on GBS type III hexasaccharide glycoconjugate. From left to right: marker, CRM_{197}, CRM_{197}-hexa low glycosylation degree **11**, CRM_{197}-hexa high glycosylation degree **12**.

Table 1. Attributes of the synthesized glycoconjugates

Glycoconjugate	mol NHS/ mol protein	Protein conc. (μg/mL)	Sacch. conc. (μg/mL)	Saccharide/protein ratio
CRM_{197}-hexa **11**	1:15	502	41.3	3.9
CRM_{197}-hexa **12**	1:50	270	44.9	7.8

The conjugates of the previously synthesized pentasaccharide units and the novel hexasaccharide were tested in mice[27] for their capability of eliciting specific anti-PSIII antibodies able to mediate opsonophagocytic killing (OPKA) of strains expressing type III PS. Two separated immunizations of BALB/c female mice were conducted by three intraperitoneal injections of the pentasaccharides (0.5 μg carbohydrate dose) and hexasaccharide (1.0 μg carbohydrate dose), respectively. All the glycoconjugates were formulated with Alum hydroxide (AlumOH) and the PSIII-CRM_{197} conjugate was used as a control for both immunizations. The animals received booster doses of the same vaccines 21 and 35 days after the first immunization. Immunogenicity of the glycoconjugates was evaluated by measurement of IgG titers by ELISA after the second and third immunization.

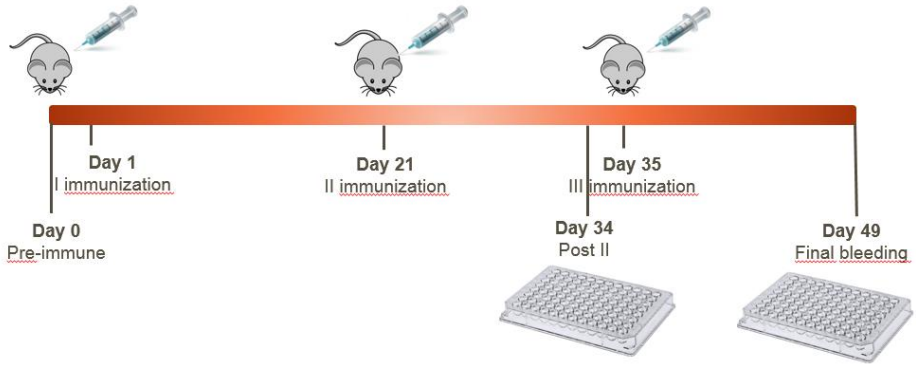

Figure 9. Immunization scheme for the CRM-oligosaccharides conjugates

As shown in Figure 10, in the first immunization with the CRM-conjugates of the GBS type III repeating unit **1**, **2** and **3** only the highly glycosylated (~23 sugar chains per mol of protein) CRM_{197} conjugate of the branched pentasaccharide **2** could elicit some anti-PS antibodies. These antibodies were also functional in the OPKA assay. No immune response was observed upon immunization with the low glycosylated conjugate of compound **2** or glycoconjugates of the linear and Y-shape repeating unit **1** and **3**. In contrast, a strong immune response was observed after 2 doses and 3 doses using the hexasaccharide-CRM_{197} conjugate having the higher saccharide/protein ratio, while no antibody titers was detected for the hexasaccharide conjugate with the lower saccharide/protein ratio. This proved that the hexasaccharide not only represents an antigenic determinant but also the minimal immunogenic epitope. The upstream glucosamine A' of the hexasaccharide proved to be crucial both for antibody recognition and for immunogenicity.

In addition, the glycosylation degree of the conjugate appeared to be a crucial parameter to elicit an immune response in mice with these relatively short synthetic oligosaccharide.

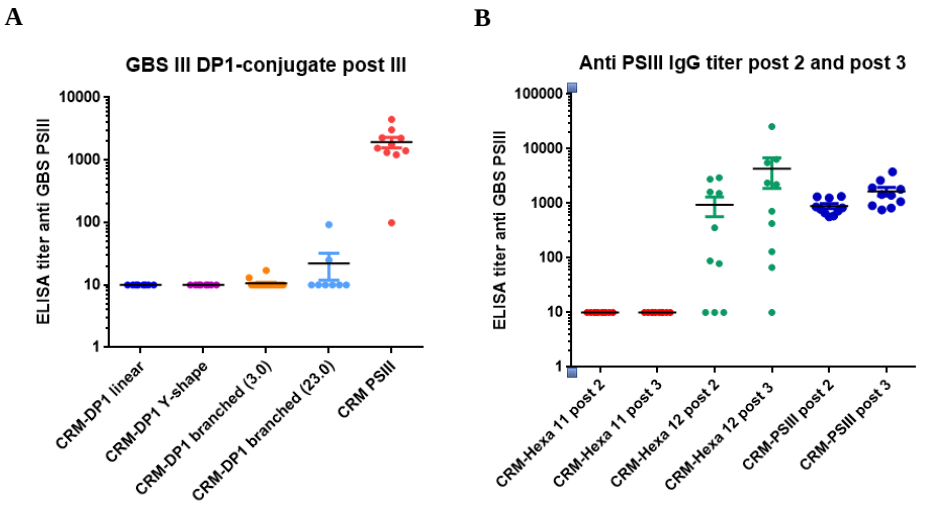

Figure 10. A) Elisa titers post III elicited by CRM_{197}-DP1 linear (in blue), CRM_{197}-DP1 Y-shape (in purple), CRM_{197}-DP1 branched 3.0 (in orange), CRM197-DP1 branched 23.0 (in light blue). CRM_{197}-PSIII (in red) was used as positive control. B) Elisa titers post II and post III elicited by CRM_{197}-hexa **11** (in red), CRM_{197}-hexa **12** (in green) and CRM_{197}-PSIII (in blue).

Antibody functional activity was assessed by an *in vitro* OPK assay which is a well-established technique to mimic the *in vivo* process of GBS killing after bacterial opsonization by effector cells in the presence of complement and specific antibodies. In this assay, sera are tested at different serial dilutions and the reported OPKA titers, expressed as the reciprocal of the serum dilution leading to 50% bacterial killing, have been shown to correlate with mouse protection levels in a passive immunization/GBS challenge models.

In agreement with the ELISA analysis, OPKA of the pooled sera after 3 doses of the high density hexa-CRM vaccine indicated good functionality of the elicited antibodies (See Table 2).

Table 2. OPKA titers post second and third immunization with glycoconjugates Hexa-CRM_{197} **12** and PSIII-CRM_{197}. Pre-immune sera were added as negative control.

Post	Vaccine	OPKA titer
Pre-immune		<30
2	Hexa-CRM_{197} **12**	<100
3	Hexa-CRM_{197} **12**	369
2	PSIII-CRM_{197}	<100
3	PSIII-CRM_{197}	420

Moreover, the level of IgM antibodies was also measured for both conjugate **12** and CRM-PSIII in mice having received two immunizations. While CRM-PSIII elicited high levels of IgMs, the

conjugated hexasaccharide induced primarily IgGs. Apparently, the long polysaccharide seems to be recognized with higher avidity by B-cell receptors, driving IgM production.

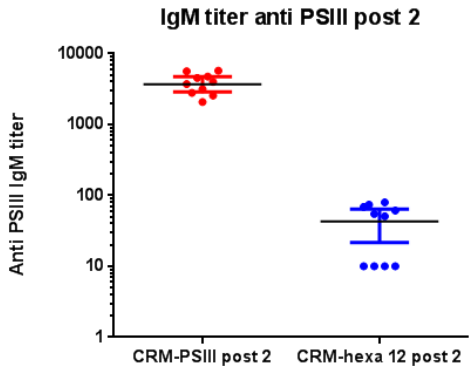

Figure 11. Elisa IgM titers after second immunization with CRM-PSIII and CRM-hexa **12**

Overall, these data suggest that the hexasaccharide fragment which is comprised within two PSIII RUs is an immunogenic epitope, in line with the minimal structure demonstrated to be necessary for antibody recognition. Furthermore, it is confirmed that the glycosylation degree plays a key role in the immune response to small carbohydrate epitopes. Indeed, only the glycoconjugate **12** with higher carbohydrate loading is able to elicit GBSIII specific functional antibodies.

Conclusion

Group B streptococcus type III is one of the serotypes which causes the highest number of GBS related diseases. Its capsular polysaccharide has always been considered a main virulence factor and target of vaccine development program. For many years, it has been considered the prototype of a length-dependent conformational glyco epitope but a recent study has shown how a fragment as long as two repeating units is able to interact with a functional anti PSIII rabbit monoclonal antibody. In particular, X-ray crystallography combined with STD-NMR of a semisynthetic PS dimer complexed with a protective mAb demonstrated the existence of a sialic acid-dependent antigenic determinant that is fully contained within six sugars (four deriving from the PSIII backbone and one from the disaccharide arm). This structure has recently been proven to be immunogenic after conjugation to carrier protein, demonstrating to contain the minimal polysaccharide epitope[10]. These findings led to design and synthesis of a hexasaccharide structure to be tested as an immunogenic mimick of the full polysaccharide.

First, the antigenic nature of the assembled hexasaccharide was confirmed by competitive SPR, where the short glycan proved to be as good an inhibitor of the binding of an anti PSIII mAb to a chip coated with PSIII-HSA as the full DP2. Furthermore, STD-NMR showed how the acetamides of the sialic acid and of the glucosamine A' were in close proximity to the mAb binding site, and

therefore likely involved in the binding. Molecular modelling simulations corroborated these observations by showing the conformational preferences of the hexasaccharide in the binding pocket of the mAb. Superimposition of the complex Fab-DP2 and the simulated mAb-hexasaccharide showed that both are very similar and share most of the contact points.

Overall, these data confirmed that the hexasaccharide is the minimal antigenic determinants recognized by a protective anti PSIII rabbit mAb. Conjugation of the hexasaccharide to the well-known carrier protein CRM_{197} allowed the evaluation of its immunogenicity *in vivo*. To this aim, two glycoconjugates to CRM_{197} were prepared to understand the impact of the glycosylation degree, that is the number of sugar chains per mol of protein, on the immune response *in vivo*. Confirming a trend that has been previously observed for short glycan antigens, only the glycoconjugate at higher glycosylation degree (about 8 chains of sugar per mol of protein) elicited a significative titer of functional antibodies comparable to the titer elicited by the positive control PSIII-CRM_{197}. An opsonophagocytic killing assay showed that these antibodies were functional. Interestingly, the immune response was not homogeneous in all animals, with some mice showing a very low antibody titer. While previous literature reports suggested GBSIII as an extremely complex epitope and pointed out the necessity of using long polysaccharide portions to contain functional epitopes, this structure guided approach counteracts this paradigm and shows that a small hexasaccharide can be designed to contain all the carbohydrate moieties needed for immunogenicity. This opens new possibilities for further improvement of synthetic vaccines based on small synthetic antigens, for instance by using a larger carrier (i.e. nanoparticles) to maximize the multivalent exposure of the epitope.

Experimental

General Methods and procedures. Reactions were monitored by thin-layer chromatography (TLC) on Silica Gel 60 F254 (Sigma Aldrich); after exam under UV light, compounds were visualized by heating with 10% (v/v) ethanolic H_2SO_4. In the work up procedures, organic solutions were washed with the amounts of the indicated aqueous solutions, then dried with anhydrous Na_2SO_4, and concentrated under reduced pressure at 30–50ºC on a water bath. Column chromatography was performed on Silica Gel 60 (Sigma Aldrich, 0.040–0.063 nm) or using pre-packed silica cartridges Reside (Teledyne-Isco, 0.040–0.063 nm) or Biotage SNAP Ultra (Biotage, silica 0.050 nm). Unless otherwise specified, a gradient 0-100% of the elution mixture was applied in a Combiflash Rf (Teledyne-Isco) or Biotage Isolera instrument. Solvent mixtures less polar than those used for TLC were used at the onset of separation. ^{1}H NMR spectra were measured at 400 MHz and 298 K with a Bruker AvanceIII 400 spectrometer; ^{1}H values are reported in ppm, relative to internal Me_4Si (^{1}H = 0.00, $CDCl_3$); solvent peak for D_2O was calibrated at 4.79 ppm. ^{13}C NMR spectra were measured at 100 MHz and 298 K with a Bruker AvanceIII 400 spectrometer; ^{13}C values are reported in ppm relative to the signal of $CDCl_3$ (^{13}C = 77.0, $CDCl_3$). Assignments of NMR signals were made by homonuclear and heteronuclear 2-dimensional correlation spectroscopy, run with the software supplied with the spectrometer. Assignment of ^{13}C NMR spectra of some compounds was aided by comparison with spectra of related substances reported previously from this laboratory or elsewhere. When reporting assignments of NMR signals, sugar residues in oligosaccharides are indicated with capital letters. Exact masses were measured by electron spray ionization cut-off spectroscopy, using a Q-Tof micro Macromass (Waters) instrument. Structures of these compounds follow unequivocally from the mode of synthesis, NMR data and *m/z* values found in their mass spectra.

[2,6-Di-O-benzoyl-3,4-O-(1-bromomethylethylidene)-β-D-galactopyranosyl)]-(1-4)-2,3,6-tri-O-benzoyl-α-D-glucopyranosyl bromide 5.

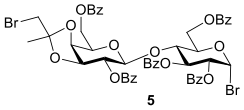

5

Ethyl thiol lactose starting material (850 mg, 0.90 mmol) was dissolved in CH_2Cl_2 (10 mL) and bromine (167 µL, 3.14 mmol) was added at 0°C. The reaction was stirred for 80 min and then quenched by the addition of triethylamine (2 mL). The solution was washed with Na_2SO_3 and water, organic phase was dried with Na_aSO_4 and evaporated under reduced pressure. The crude was finally purified by flash chromatography (toluene +3% TEA:Acetone) to afford **5** as a white solid in 75% yield (704 mg, 0.68 mmol). ESI MS m/z $[M-Br]^+$ found 964.6761; calcd 963.7834

^{1}H NMR (400 MHz, $CDCl_3$): δ 8.02-7.20 (m, 25H, H-Ar), 6.64 (d, J=3.68, 1H, H-1^A), 5.99 (t, 1H, H-3^A), 5.15-5.09 (m, 2H, H-2^A, H-2^B), 4.66 (d, J=7.06, 1H, H-1^B), 4.51 (dd, 2H, H-6$_{a,b}$), 4.39-4.34 (m, 2H, H-4^B), 4.28 (d, 1H), 4.21 (t, 1H), 4.14 (m, 1H, H-6$_a$), 3.78 (m, 2H, H-6$_b$), 3.22 (q, 2H, (C(CH_3)(CH_2Br)), 1.51 (s, 3H, (C(CH_3)(CH_2Br)).

^{13}C NMR (101 MHz, $CDCl_3$): d 128.4–133.8 (C-Ar), 109.4 (*C*(CH3)(CH2Br)), 100.5 (C -1$_B$), 86.9 (C-1$_A$), 78.0, 74.6, 74.5, 73.5, 73.2, 71.6, 71.2, 70.3, 62.7, 61.8, 37.2 (C(CH3)(*C*H2Br)), 24.5 (C(*C*H3)(CH2Br)).

3-Azidopropyl 2,4,6-tri-*O*-benzoyl-3-*O*-(methyl 4,7,8,9-tetra-*O*-acetyl-5-*N*-acetamido-3,5-dideoxy-D-glycero-α-D-galacto-non-2-ulopyranosylonate)-β-D-galactopyranosyl)-(1→4)-3-*O*-benzyl-2-deoxy-2-phthalimido-β-D-glucopyranoside 6

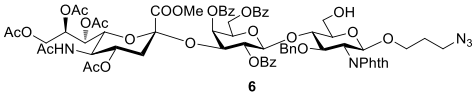

6

Compound **6** was synthesized as previously reported[20]; ^{1}H NMR and ^{13}C NMR are in line with ones reported in literature[20].

3-Azidopropyl [2,6-di-O-benzoyl-3,4-O-(1-bromomethylethylidene)-β-D-galactopyranosyl-(1-4)-2,3,6-tri-O-benzoyl-β-D-glucopyranosyl-(1-6)]-[2,4,6-tri-O-benzoyl-3-O-(methyl 4,7,8,9-tetra-O-acetyl-5-N-acetamido-3,5-dideoxy-D-glycero-α-D-galacto-non-2-ulopyranosylonate)-β-D-galactopyranosyl-(1-4)]-3-*O*-benzyl-2-deoxy-2-phthalimido-β-D-glucopyranoside 7.

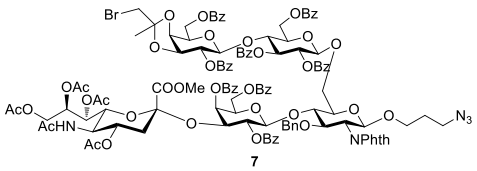

7

A solution of trisaccharide acceptor **6** (330 mg, 0.24 mmol) and donor **5** (420 mg, 0.60 mmol) with activated molecular sieves (4 A, 800 mg) in DCM (8 mL) was stirred for 20 min under nitrogen. AgOTf (77 mg, 0.30 mmol) was added at -40 °C. The reaction mixture was stirred for 10h at rt, when TLC (7:3 Toluene:acetone) showed complete reaction. TEA was added, the solid filtered off and the solvent removed at reduced pressure. The crude was purified by flash chromatography (Toluene:acetone 8:2) to afford **7** (370 mg, 0.16 mmol) in 65% yield. yield. $[\alpha]_D^{25} = +42.73^\circ$ (c 1.4, CHCl3). ESI MS m/z $[M+H]^+$ found 2395.1274; calcd 2395.1439.

^{1}H NMR (400 MHz, $CDCl_3$) δ 8.08-6.58 (m, 49H, H-Ar), 5.71 (t, J = 8.90 Hz, 1H, H-8^C), 5.45-5.37 (m, 2H, H-2^B, H-3^D), 5.22-5.14 (m, 3H, H-2^D, H-4^B, H-2^E), 5.07 (dd, J = 2.84, 9.86 Hz, 1H, H-7^C), 4.92 (d, J=10.2, 1H, NH), 4.82-4.68 (m, 5H, H-1^A, H-1^B, H-3^B, H-4^C, C*H*HPh^A), 4.42 (d, J=7.22, 1H, H-1^E), 4.39-4.24 (m, 5H), 4.20- 4.16 (m, 2H, H-1^D, CH*H*Ph^A), 4.05 (dd, J = 5.35, 11.22 Hz, 1H, H-9^C), 3.97-3.86 (m, 6H), 3.73 (m, 6H), 3.63-3.42 (m, 7H, incl. OCH_{2a}), 3.25 (q, J=8.69, 2H, C*H*$_2$Br), 3.10-3.05 (m, 1H, OCH_{2b}), 2.91-2.84 (m, 2H, C*H*$_2$N$_3$), 2.77-2.73 (m, 1H, H-5^E), 2.38 (dd, 1H, H-3^C_e), 2.03, 1.75, 1.71, 1.66, 1,53 (5 x s, 3H each, 5 x C*H*$_3$CO), 1.60 [s, 3H, C(C*H*$_3$)], 1.54 (m, 1H, H-3^C_a), 1.37-1.28 (m, 2H, OCH_2CH_2).

^{13}C NMR (101 MHz, $CDCl_3$) δ 170.80-164.89 (13x C=O esters) 134.20-122.37 (m, 49, C-Ar), 101.88 (C-1^D), 100.99 (C-1^B), 100.54 (C-1^E), 97.93 (C-1^A), 96.87, 80.25, 78.18, 78.03, 75.68, 74.97, 74.62, 74.56, 73.39, 72.70, 72.45, 72.72, 72.58, 72.52, 72.43, 71.06, 70.58, 70.41, 69.46, 68.16, 67.54, 67.02, 66.85, 66.18, 63.21, 62.21, 62.76, 62.33, 61.55, 55.76, 53.23, 48.62, 48.01, 37.31 (C-3^C), 37.07, 28.62, 24.58, 23.14, 21.33, 20.75, 20.73, 20.43.

3-Azidopropyl [2,6-di-*O*-benzoyl-β-D-galactopyranosyl-(1-4)-2,3,6-tri-*O*-benzoyl-β-Dglucopyranosyl-(1-6)]-[2,4,6-tri-*O*-benzoyl-3-*O*-(methyl 4,7,8,9-tetra-*O*-acetyl-5-*N*-acetamido-3,5-dideoxy-D-glycero-*α*-D-galacto-non-2-ulopyranosylonate)-β-D-Galactopyranosyl-(1-4)]-3-*O*-benzyl-2-deoxy-2-phthalimido-β-D-glucopyranoside 8.

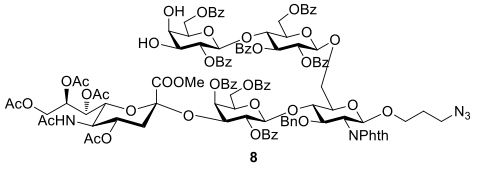

8

Pentasaccharide **7** (370 mg, 0.16 mmol) was dissolved in a 90% solution of TFA. After 1h at rt, TLC (Toluene:Acetone 6:4) showed complete reaction. Reaction was concentrated under reduced pressure and purified via flash chromatography (Toluene:acetone 7:3) giving **8** (302 mg, 0.13 mmol) in 83% yield as a white solid.

$[\alpha]_D^{25} = +38.78^\circ$ (c 1.5, CHCl3). ESI MS m/z $[M+H]^+$ found 2276.9871; calcd 2277.1840.

^{1}H NMR (400 MHz, CDCl3) δ 8.08-6.58 (m, 49H, H-Ar), 5.69 (t, J = 8.90 Hz, 1H, H-8^C), 5.46-5.38 (m, 2H, H-2^B, H-3^D), 5.26-5.17 (m, 3H, H-2^D, H-2^E, H-4^B), 5.08 (dd, J = 2.36, 9.81 Hz, 1H, H-7^C), 4.98 (d, J = 10.07, 1H, NH), 4.80-4.68 (m, 5H, H-1^B, H-1^A, H-4^C, H-3^B, C*H*HPh), 4.45 (d, J = 7.81, 1H, H-1^E), 4.39-4.32 (m, 2H, H-9^C_a, H-6^E_a), 4.26 (d, J = 7.64, 1H), 4.13 (d, J = 12.25, 1H, CH*H*Ph), 3.97-3.85 (m, 9H, incl. H-2^A, H-4^E), 3.72 (m, 6H, incl. H-5^C, H-9^C_b, $COOCH_3$), 3.64-3.59 (m, 3H), 3.56-3.44 (m, 5H, incl. OCH_{2a}), 3.16-3.10 (m, 1H, OCH_{2b}), 2.91 (q, J = 6.04, 2H), 2.83-2.79 (m, 1H), 2.37 (dd, J = 4.62, 12.79, 1H, H-3^C), 2.01, 1.83, 1.70, 1.67, 1.52, (5 x s, 3H each, 5 x CH_3CO), 1.46 (m, 1H, H-3^C), 1.36 (m, 2H, OCH_2CH_2)

^{13}C NMR (101 MHz, $CDCl_3$) δ 170.0-164.9 (13x C=O esters), 134.0-125.1 (C-Ar), 101.66 (C-1^D), 101.04 (C-1^B), 100.98 (C-1^E), 97.93 (C-1^A), 96.89, 80.15, 74.95, 74.57, 73.69, 72.99, 72.51, 72.39, 71.68, 71.58, 71.45, 70.58,

70.09, 69.48, 68.17, 67.00, 66.86, 66.19, 63.14, 62.91, 61.70, 61.53, 55.74, 53.24, 48.61, 48.02, 46.71, 37.31 (C-3^C), 28.64, 23.13, 21.33, 20.75, 20.72, 20.45.

3-Azidopropyl [3-*O*-benzyl-4,6-O-benzyliden-2-deoxy-2-phthalimido-β-D-glucopyranosyl-(1-3)-2,6-di-*O*-benzoyl-β-D-galactopyranosyl-(1-4)-2,3,6-tri-*O*-benzoyl-β-Dglucopyranosyl-(1-6)]-[2,4,6-tri-*O*-benzoyl-3-*O*-(methyl 4,7,8,9-tetra-*O*-acetyl-5-*N*-acetamido-3,5-dideoxy-D-glycero-α-D-galacto-non-2-ulopyranosylonate)-β-D-galactopyranosyl-(1-4)]-3-*O*-benzyl-2-deoxy-2-phthalimido-β-D-glucopyranoside 10.

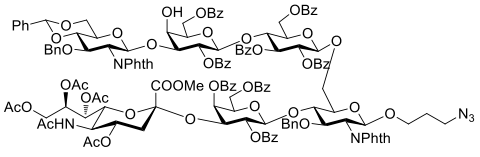

10

A solution of Glucosamine donor **9** (68 mg, 0.11 mmol) and acceptor **7** (190 mg, 0.08 mmol) was stirred for 20 min in dry DCM with activated molecular sieves 4Å under nitrogen. TfOH was then added at -25°C and the reaction was stirred for 1h at 0°C. After that, TLC (Toluene:Acetone 6:4) showed complete reaction, so the mixture was quenched with TEA, the solid was filtered off and the crude was purified with flash chromatography. Hexasaccharide **10** (164 mg, 0.06 mmol) was obtained has a white solid in 69% yield.

$[\alpha]_D^{25}$ = + 36.31° (c 0.32, CHCl3). ESI MS m/z $[M+H]^+$ found 2745.8362; calcd 2745.6693.

^{1}H NMR (400 MHz, $CDCl_3$) δ 8.04-6.61 (m, 63H, H-Ar), 5.73 (t, J = 9.09, 1H, H-8^C), 5.55 (s, 1H, C*H*Ph), 5.46 (t, J = 8.46, 1H, H-2^B), 5.30-5.10 (m, 6H, H-1^F, H-3^D, H-2^D, H-2^E, H-4^B, H-7C), 4.91 (d, J = 10.04, 1H, NH), 4.79-4.68 (m, 6H, H-1^B, H-1^A, C*H*HPh^A, C*H*HPh^F), 4.36-4.22 (m, 6H, incl. H-1^E), 4.12-4.03 (3H), 3.98-3.87 (m, 7H, incl. H-1^D), 3.83-3.67 (m, 11H), 3.62-3.47 (m, 8H, OCH_{2a}), 3.14-3.08 (m, 1H, OCH_{2b}), 2.94-2.90 (m, 2H, C*H*$_2$N$_3$), 2.49-2.40 (m, 2H, H-3^C, H-5^E), 2.06, 1.91, 1.77, 1.67, 1.59 (5 x s, 3H each, 5 x C*H*$_3$CO), 1.58 (m, 1H, H-3^C), 1.37 (m, 2H, C*H*$_2$CH$_2$N$_3$)

^{13}C NMR (101 MHz, $CDCl_3$) δ 170.80-164.24 (13 x C=O esters), 138.00-125.11 (C-Ar), 102.04 (C-1^D), 101.36 (*C*HPh), 101.01 (C-1^B), 100.88 (C-1^E), 99.98 (C-1^F), 97.88 (C-1^A), 82.66, 80.59, 80.53, 78.12, 75.57. 75.01, 74.43, 74.18, 74.03, 72.45, 72.33, 72.06, 71.67, 71.54, 71.42, 71.33, 70.82, 70.64, 70.47, 69.53, 98.53, 68.40, 68.14, 67.07, 66.80, 66.23, 66.11, 63.25, 62.71, 62.46, 61.50, 55.73, 55.50, 53.25, 48.57, 48.03, 37.36 (C-3^C), 28.59, 23.13, 21.49, 21.32, 20.77, 20.34.

3-Aminopropyl 3-O-(5-N-acetamido-3,5-dideoxy-D-glycero-α-D-galacto-non-2-ulopyranosyl)-β-D-galactopyranosyl)-(1→4)-O-[(2-acetamido-2-deoxy-β-D-glucopyranosyl)-(1→3)-(β-D-galactopyranosyl)-(1→4)-O-(β-D-glucopyranosyl)-(1→6)]-O-2-acetamido-2-deoxy-β-D-glucopyranoside 4.

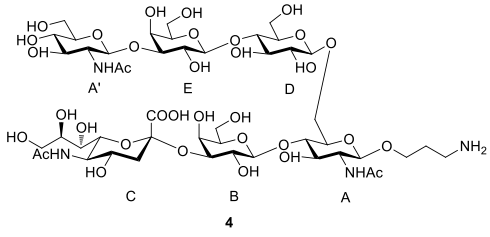

4

A mixture of protected hexasaccharide **10** (0.1 mmol) and LiI (3 mmol) in pyridine (5 mL) was heated for 24h at 120 °C. The reaction mixture was concentrated under vacuum, and the residue was purified by silica gel column chromatography (gradient 2% MeOH in DCM) to afford the demethylated product. This material was dissolved in ethanol (4 mL), and ethylenediamine (400 µL) was added. After being stirred for 16 h at 90 °C, the reaction mixture was then concentrated in vacuo, and the residue was coevaporated with Toluene (2 x 10 mL) and EtOH (2 x 5 mL). The crude mixture was re-dissolved in pyridine (5 mL), and acetic anhydride (5 mL) was added. After being stirred for 16 h at rt, the reaction mixture was concentrated under reduced pressure and the residue was purified by silica gel column chromatography (gradient 10 % of MeOH in DCM). The residue was dissolved in MeOH and MeONa was added until pH=13.

After 48 h the reaction was neutralized and the solvent removed under vacuum and the crude was purified with C18 5g column (gradient 20% MeOH in H_2O). The residue was finally dissolved in MeOH and Pd/C (1:1 w/w in respect to the sugar) was added. The reaction mixture was stirred under pressure of H_2 (3 bar) for 72 h. Then, the catalyst

was filtered off and the filtrate concentrated under reduced pressure. The reaction mixture was purified by G-10 size-exclusion column chromatography using water for elution.

Fractions containing the sugar were quantified by sialic acid assay and freeze-dried to afford the deprotected oligosaccharide **4** as an amorphous powder (31 % yield).

$[\alpha]_D^{25}$ = +1.56° (c 0.81, H_2O). ESI MS m/z $[M+Na]^+$ found 1281,4932; calcd 1281,4610.

^{1}H NMR (400 MHz, D_2O) δ 4.68 (d, J = 8.4 Hz, 1H, H.1^F), 4.60 (d, J= 7.9 Hz, 1H, H-1^B), 4.53 (d, J= 8.49 Hz, 1H, H-1^D), 4.50 (d, J= 8.63 Hz, H1, H-1^A), 4.43 (d, J= 7.77 Hz, 1H, H-1^E), 4.30, (d, J= 10.5 Hz, 1H, H-6$^A{}_a$), 4.14 (d, J= 2.7 Hz, 1H, H-4^E), 4.08, (dd, J= 2.7, 9.8 Hz, 1H, H-3^B), 3.99-3.80 (8H), 3.79-3.54 (22H), 3.46-3.44 (2H), 3.34 (t, J= 8.2 Hz, 1H, H-2^E), 3.20 (t, J= 8.6 Hz, 2H, C*H*$_2$N$_3$), 2.75, (dd, J= 4.6, 12.4 Hz, 1H, H-3$^C{}_{eq}$), 2.03 (s, 6H, 2 x CH_3CO), 2.02 (s, 3H, CH_3CO), 1.97 (m, 2H, C*H*$_2$CH$_2$N$_3$), 1.80 (t, J= 12.4 Hz, 1H, H-3$^C{}_{ax}$).

^{13}C NMR (101 MHz, D_2O) δ 102.91 (C-1^E), 102.81 (C-1^F), 102.42 (C-1^D), 102.12 (C-1^B), 101.33 (C-1^A), 81.87, 78.20, 77.25, 75.60, 75.00, 74.85, 74.58, 74.24, 73.50, 75.44, 72.91, 72.62, 72.08, 71.75, 69.98, 69.93, 69.33, 68.33, 67.98, 67.51, 67.30, 62.56, 61.05, 60.93, 60.42, 59.99, 55.60, 55.01, 51.63, 49.09, 47.37, 39.59 (C-3^C), 23.52, 22.11, 22.01.

SPR Fab binding inhibition

Inhibition assay were performed by SPR using a BIACORE X100 system. HSA-PSIII Glycoconjugate was immobilized on CM5 sensor chips (Biacore) using the amine coupling kit supplied by the manufacturer (Biacore). Immobilizations were conducted in 10-20 mM sodium acetate (pH 4-5) at sugar concentrations of 2-4 μg/mL. The immobilized surface density was ~50 resonance units in each instance. Binding analysis was performed with samples of Fab at a fixed concentration pre-incubated with PSIII or its fragments serially diluted (2x) starting from a concentration of 2 mg/mL. Measurements were conducted in 10 mM HEPES (pH 7.2), 150mM NaCl, 3 mM EDTA, 0.005% Tween 20 at 25°C and at a flow rate of 45μL/min. Following mAb or Fab binding, conjugate surfaces were regenerated with 3.5M $MgCl_2$ and a contact time of 120 s. Sensorgram data were analyzed using BIAevaluation software (Biacore).

NMR Sample preparation

mAb were exchanged in the working buffer (Tris d-11 50 mM in D_2O at pH 8.0 +/- 0.1) through 2 mL Zeba Spin desalting column saturated with 3 cycles of working buffer, mAb were finally eluted at the same starting concentration of 1 mg/ml. The 100% of recovery was assessed through microBCA spectrophotometric assay. Hexasaccharide fragment was desalted, quantified, dried and then dissolved in the working buffer too. mAb final concentration in the NMR tube was of 4 μM. mAb:ligand (saccharide) ratio was set at 1:50 mol/mol.

STD NMR experiments

NMR experiments were carried out on a Bruker 600 MHz NMR instrument equipped with a QCI cooled probe at controlled temperature (± 0.1 K). Data acquisition and processing were performed using TOPSPIN 3.5 software, respectively. Suppression of water signal was achieved by excitation sculpting (2 msec selective square pulse). STD-NMR experiments were acquired with 72 scans over 72 accumulations and spectral width of 9600 Hz (16 ppm) at 303 K; a saturation transfer of 0,5/1/1,5/2/4 sec. was applied to enhance the saturation transfer effect, irradiating at a frequency of 8.0 and -1.0 ppm (2 different spectra recorded for each sample). No differences were observed in the STD spectra irradiating at 8.0 or -1.0 ppm (4800 and -600 Hz respectively) for all samples, confirming that the saturation transfer effect was not irradiation dependent. To avoid pitfalls in the interpretation of STD-NMR spectra, a negative control spectrum was always recorded in absence of mAb (ligand and buffer) at the very same condition (concentration and pH) of the mAb-saccharide samples. Increasing saturation times from 0.5 up to 4.0 sec were applied to avoid overseeing of possible bias in the calculation of STD effects due to the different proton longitudinal relaxation times (T1), as well as the intramolecular spin diffusion within the bound state.

Conjugation to CRM_{197}

Triethylamine (3.0 eq) was added to a 9:1 DMSO/water solution of hexasaccharide, followed by di-N-hydroxysuccinimidyl adipate (12 eq). The reaction was stirred for 3 h, then the product was precipitate at 0°C by adding ethyl acetate (9 volumes). The solid was washed 10 times with ethyl acetate (5 volumes each) and lyophilized. The activated sugar was conjugated to CRM197 in sodium phosphate 100 mM at a protein concentration of 20 mg/mL, using the mol saccharide/mol protein ratio reported in Table 1.

After incubating overnight, the glycoconjugates **11** and **12** were purified by dialysis against 10 mM sodium phosphate buffer pH 7.2 (30 washings) in 30 kDa Vivaspin Turbo (Sartorius) centrifugal concentrators and reconstituted in the same buffer.

SDS-PAGE was performed on 4–12 % pre-casted polyacrylamide gel (NuPAGE®Invitrogen) using MOPS 1x as running buffer (NuPAGE®Invitrogen). 5 μg of protein were loaded for each sample. After electrophoretic running with a voltage of 150 V for about 45 min, the gel was stained with blue Coomassie.

HPAEC-PAD analysis for revealing Gal, Glc and GlcNAc

Standard samples of GBS PSIII at five increasing concentrations ranging between 0.5 and 10.3 μg/mL were prepared to build the calibration curve. GBS PSIII samples were prepared targeting the calibration curve midpoint. The reference and analytical samples were prepared in 4 M trifluoracetic acid, incubated at 100°C for 3h, dried under vacuum (SpeedVac Thermo), and suspended in water. All analytical samples were filtered with 0.45 μm Phenex-NY (Phenomenex) filters before analysis. HPAEC-PAD analysis was performed with a Dionex ICS-3000 equipped with a CarboPac PA1 column (4 × 250 mm; Dionex) coupled with a PA1 guard to column (4 × 50 mm; Dionex). Samples (50 μL injection volume) were run at 1 mL/min, using isocratic elution with 14 mM NaOH, followed by a washing step with 0.5 M NaOH.

HPAEC-PAD data acquisition and analysis

In HPAEC-PAD analysis, the effluent was monitored using an electrochemical detector in the pulse amperometric mode with a gold working electrode and an Ag/AgCl reference electrode. A quadruple-potential waveform for carbohydrates was applied. The resulting chromatographic data were processed using Chromeleon software 6.8 (Dionex). Gal, Glc, GlcNAc and Neu5Ac concentration were determined and converted in μmol/mL to estimate the relative mol/mol ratio.

Immunogenicity of conjugates in mice

Two groups of ten female BALB/c mice were immunized by intraperitoneal injection of 1 μg in saccharide content of each produced glycoconjugate using alum hydroxide as an adjuvant. CRM-PSIII were used as controls. Mice received the vaccines at days 1, 21 and 35. Sera were bled at days 1, 35 and 49.

ELISA analysis using unconjugated PSIII as coating reagent

Microtiter plates (96 wells, NUNC, Maxisorp) were coated with 100 μL of unconjugated PS III in PBS pH 7.4 (35μg/mL), followed by overnight incubation at 2-8°C. After washing three times with PBST, a PBS solution containing 2% BSA and sucrose (51 mg/mL) was added (250 μL/well), and plates were incubated 90 min at 37°C, and then aspirated to remove the solution. Two-fold serial dilutions of test and standard sera in PBST-B were added to each well. Plates were then incubated at 37°C for 2 hours, washed with PBST, and incubated for 2 additional hours at 37°C with either anti-mouse IgG-alkaline phosphatase (Sigma) diluted 1:2000 in PBST-B. After washing, the plates were developed with a 4 mg/mL solution of *p*-Nitrophenyl Phosphate (pNPP) in 1 M diethanolamine (DEA) pH 9.8, at rt for 30 min. After blocking with 7 % EDTA, the absorbance values measured with a SPECTRAmax plate reader with wavelength set at 405 nm. IgG concentrations were calculated as reciprocal serum dilution giving OD of 1.0.

ELISA analysis using GBS PS III conjugated to human serum albumin (HSA) as coating reagent

Microtiter plates (96 wells, NUNC, Maxisorp) were coated with 100 µL of 1µg/mL of GBS PSIII conjugated to HSA *via* the spacer adipic acid dihydrazide in Phosphate Buffered Saline (PBS) pH 7.4. Plates were incubated overnight at 2-8°C, washed three times with PBST (0.05% Tween-20 in PBS pH 7.4) and saturated with 250 µL/well of PBST-B (2% Bovine Serum Albumin-BSA in PBST) for 90 min at 37°C. The plates were then aspirated to remove the solution. Two-fold serial dilutions of test and standard sera in PBST-B were added to each well. Plates were then incubated at 37°C for 1h, washed with PBST, and then incubated for 90 min at 37°C with anti-mouse IgG or IgM - alkaline phosphatase (Sigma) diluted 1:2000 or anti-rabbit IgG-alkaline phosphatase diluted 1:1000 in PBST-B. After washing, the plates were developed with a 4 mg/mL solution of p-Nitrophenyl Phosphate (pNPP) in 1 M diethanolamine (DEA) pH 9.8, at rt for 30 min. After blocking with 7% EDTA, the absorbance was measured using a SPECTRAmax plate reader with wavelength set at 405 nm. IgG concentrations were expressed as relative ELISA Units/mL (EU/mL) and were calculated by interpolating the absorbance values of serial sample dilutions on the standard calibration curve (Reference line method). The murine standard consists of a pool of hyperimmune sera obtained from animals immunized with 3 doses of GBS PS III-CRM conjugate vaccines adjuvanted with Alum.

Opsonophagocytic Killing Assay (OPKA)

Functional activity of anti-GBS antibodies was estimated by Opsono Phagocytic Killing Assay (OPKA) using differentiated HL-60 cells and strains COH1-III[2]. The percent of killing was calculated as (mean Colony Forming Units at T0 - mean CFU at T60)/(mean CFU at T0). OPK titers were expressed as the reciprocal serum dilution mediating 50% bacterial killing, estimated through piecewise linear interpolation of the dilution-killing OPK data. The Lower Limit of Detection was 1:30 and the assay coefficient of variation was approximately 30%.

References and notes

1. Kasper, D.L.; Baker, C.J.; Baltimore, R.S.; Crabb, J.H.; Schiffman, G.; Jennings, H.J. *J. Exp. Med.* **1979**, *149*, 327-339.
2. Nuccitelli, A.; Rinaudo, D.C.; Maione, D. *Ther. Adv. Vaccines*, **2015**, *3*, 76-90.
3. Seale, A.C.; Bianchi-Jassir, F.; Russell, N.J.; Kohli-Lynch, M.; Tann, C.J.; Hall, J.; Madrid, L.; Blencowe, H.; Cousens, S.; Baker, C.J.; Bartlett, L.; Cutland, C.; Gravett, M.G.; Heath, P.T.; Ip, M.; Le Doare, K.; Madhi, S.A.; Rubens, C.E.; Saha, S.K.; Schrag, S.J.; Sobanjo-Ter Meulen, A.; Vekemans, J.; Lawn, J.E. *Clin. Infect. Dis.* **2017**, *65*, S200-S219.
4. Morven, C.J.B.; Edwards, S. *Aging Infect. Dis.* **2005**, *41*, 839–847.
5. Song, J.Y.; Lim, J.H.; Lim, S.; Yong, Z.; Seo, H.S. *Hum. Vacc. Immunother.* **2018**, *14*, 2669-2681.
6. Kasper, D.L.; Baker, C.J. *N. Engl. J. Med.* **1976**, *294*, 753-756.
7. Paoletti, L.C.; Kasper, D.L.; Michon, F.; DiFabio, J.; Holme, K.; Jennings, H.J.; Wessels, M.R. *J. Biol. Chem.* **1990**, *265*, 8278-18283.
8. Michael, V.P.; Wessels, M.R.; Kasper, D.L.; Jennings, H.J. *J. Biol. Chem.* **1987**, *262*, 8262-8267.
9. Donders, G.G:; Halperin, S.A.; Devlieger, R.; Baker, S.; Forte, P.; Wittke, F.; Slobod, K.S.; Dull, P.M. *Obstet. Gynecol.* **2016**, *127*, 213-221.
10. Carboni, F.; Adamo, R.; Fabbrini, M.; De Ricco, R.; Cattaneo, V.; Brogioni, B.; Veggi, D.; Pinto, V.; Passalacqua, I.; Oldrini, D.; Rappuoli, R.; Malito, E.; Margarit Y Ros, I.; Berti, F. *Proc. Natl. Acad. Sci. U. S. A.* **2017**, *114*, 5017-5022.
11. Brisson, J.R.; Uhrinova, S.; Woods, R.J.; van der Zwan, M.; Jarrell, H.C.; Paoletti, C.; Kasper, D.; Jennings, H. *Biochemistry*, **1997**, *36*, 3278-3292.
12. Gonzalez-Outeirino, J.; Kadirvelraj, R.; Woods, R.J. *Carbohyd. Res.* **2005**, *340*, 1007-1018.
13. Jennings, H.; Lugowski, C.; Kasper, D. *Biochemistry*, **1981**, *20*, 4511-4518.
14. Zou, W.; Mackenzie, R.; Thérien, L.; Hirama, T.; Yang, Q.; Gidney, M.A.; Jennings, H. *J. Immunol.* **1999**, *163*, 820-825.
15. Kuttel, M.; Ravenscroft, N. *Pharmaceuticals*, 2019, **12**, 28.
16. Zou, W.; Jennings, H.J. *The Molecular Immunology of Complex Carbohydrates*, **2001**, pp 473-484.
17. Woods, R.J.; Yongye, A.B.; **2012**, *Computational Techniques Applied to Defining Carbohydrate Antigenicity*, ed SpringerWienNewYork, pp. 361-383.
18. Jennings, H.J.; Katzenellenbogen, E.; Lugowski, C.; Michon, F.; Roy, R.; Kasper, D.L. *Pure Appl. Chem.* **1984**, *56*, 893-905.
19. Cattaneo, V.; Carboni, F.; Oldrini, D.; De Ricco, R.; Donadio, N.; Margarit Y Ros, I.; Berti, F.; Adamo, R. *Pure Appl. Chem.* **2017**, *89*, 855-875.

20. Carboni, F.; Angiolini, F.; Fabbrini, M.; Brogioni, B.; Corrado, A; Berti, F.; Adamo, R.; Margarit, I. *J. Infect. Dis.* **2019**, DOI: 10.1093/infdis/jiz551.
21. Mayer, M.; Meyer, B. *J. Am. Chem. Soc.* **2001**, *123*, 6108-6117.
22. Meyer, E.A.; Castellano, R.K.; Diederich, F. *Angew. Chem. Int. Ed.* **2003**, *42*, 1210-1250.
23. Broecker, F.; Hanske, J.; Martin, C.E.; Baek, J.Y.; Wahlbrink, A.; Wojcik, F.; Hartmann, L.; Rademacher, C.; Anish, C.; Seeberger, P.H. *Nat. Commun.* **2016**, *7*, 11224.
24. Bernardi, A.; Jimenez-Barbero, J.; Casnati, A.; De Castro, C.; Darbre, T.; Fieschi, F.; Finne, J.; Funken, H.; Jaeger, K.E.; Lahmann, M.; Lindhorst, T.K.; Marradi, M.; Messner, P.; Molinaro, A.; Murphy, P.V.; Nativi, C.; Oscarson, S.; Penades, S.; Peri, F.; Pieters, R.J.; Renaudet, O.; Reymond, J.L.; Richichi, B.; Rojo, J.; Sansone, F.; Schaffer, C.; Turnbull, W.B.; Velasco-Torrijos, T.; Vidal, S.; Vincent, S.; Wennekes, T.; Zuilhof, H.; Imberty, H. *Chem. Soc. Rev.* **2013**, *42*, 4709-4727.
25. Adamo, R.; Romano, M.R.; Berti, F.; Leuzzi, R.; Tontini, M.; Danieli, E.; Cappelletti, E.; Cakici, O.S.; Swennen, E.; Pinto, V.; Brogioni, B.; Proietti, D.; Galeotti, C.L.; Lay, L.; Monteiro, M.A.; Scarselli, M.; Costantino, P. *ACS Chem. Biol.* **2012**, *7*, 1420-1428.
26 Adamo, R.; Nilo, A.; Castagner, B.; Boutureira, O.; Berti, F.; Bernardes, G.J. *Chem. Sci.* **2013**, *4*, 2995-3008.
27 All animal studies were ethically reviewed and carried out in accordance with European Directive 2010/63/EEC and the GSK policy on the Care, Welfare and Treatment of Animals.